Vibrational spectroscopic study of ionic liquids: Comparison between monocationic and dicationic imidazolium ionic liquids

Taqiyeddine Moumene [a,b], El Habib Belarbi [b], Boumediene Haddad [b], Didier Villemin [c], Ouissam Abbas [d], Brahim Khelifa [e], Serge Bresson [e,*]

[a] Laboratoire de Génie Énergétique et Génie Informatique L2GEGI, Université de Ibn Khaldoune, Tiaret, Algeria
[b] Laboratoire de Synthèse et Catalyse Tiaret LSCT, Université de Ibn Khaldoune, Tiaret, Algeria
[c] LCMT, ENSICAEN, UMR 6507 CNRS, Université de Caen, 6 bd Ml Juin, 14050 Caen, France
[d] Centre Wallon de Recherche Agronomique, CRA-W, Bâtiment Maurice Henseval, Chaussée de Namur, 24, 50030 Gembloux, Belgium
[e] Laboratoire de Physique des Systèmes Complexes, Université Picardie Jules Verne, 33 Rue St Leu, 80039 Amiens Cedex, France

HIGHLIGHTS

- Synthesis of dicationic ionic liquid [M(CH$_2$)IM^{2+}][2NTf$_2^-$].
- FTIR/ATR and FT-RAMAN spectroscopy study of the previous dicationic ionic liquid.
- Comparison between our dicationic ionic liquid and a monocationic ionic liquid.
- There are more active modes in FT-Raman than in FTIR/ATR spectroscopy.
- The passage from mono to dicationic is responsible of important vibrational changes.

GRAPHICAL ABSTRACT
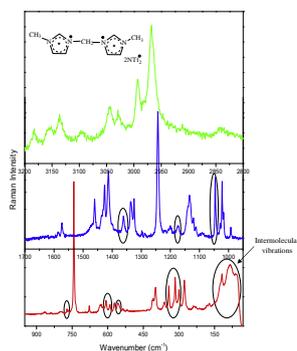
ABSTRACT

In this study, we synthesised a dicationic ionic liquids labeled bis-methyl imidazolium methylidene bis (trifluoromethanesulfonyl) imide ([M(CH$_2$)IM^{2+}][2NTf$_2^-$]). The structure was identified by NMR. In order to characterise this ionic liquid, vibrational spectroscopy studies were performed by FTIR/ATR and FT-Raman spectroscopies. A comparative study was introduced by FTIR/ATR and FT-Raman spectroscopies, between our synthesised dicationic ionic liquid and a monocationic ionic liquid ([EMIM$^+$][NTf$_2^-$]), where the anion and the cation are similar.

FTIR/ATR spectra of dicationic ionic liquid are richer in modes especially in the spectral range of 3000 cm^{-1}. In the 1400–900 cm^{-1} spectral region, the mode corresponding to the vibration of the NTf$_2^-$ anion at 1040, 1140 and 1340 cm^{-1} is very sensitive by the number of cation change. It was also the case for the peak at 1575 cm^{-1} assigned to ring in-plane symmetric/anti-symmetric stretch CH$_2$(N) and CH$_3$(N)CN stretch. In the 4000–2800 cm^{-1} spectral region, we observed few new peaks for [M(CH$_2$)IM^{2+}] comparatively with [EMIM$^+$]; a splitting for the peak at 3105 cm^{-1} and some wavenumber shifts for various modes.

For the FT-Raman spectroscopy study, we realised our study in the spectral region 4000–0 cm^{-1} while that of the monocationique sample is realised in the spectral region 1700–200 cm^{-1}. We observe in the common region 19 new peaks with the passage from the mono to dicationic, what is consequent. The impact of the passage from mono to dicationic is more important for the anion contribution spectral

* Corresponding author. Tel.: +33 623301326.
  E-mail address: sergebresson@u-picardie.fr (S. Bresson).

range (1400–300 cm^{-1}) than in the FTIR/ATR spectroscopy study. Other markers of differentiation between **[M(CH$_2$)IM^{2+}]** and **[EMIM$^+$]** are observed for vibrational modes assigned to CH$_2$(N) and CH$_3$ (N)CN stretch. We can also notice a contrast between the two spectroscopies: there are more active modes in FT-Raman than in FTIR/ATR spectroscopy.

1. Introduction

Room temperature ionic liquids (RTILs) are molten salts at room temperature. They represent a new generation of solvents. Many researches have been developed the last years on these products because of their interesting properties such as: low melting temperature ($T_f < 100$), low vapour pressure, the easiness in regenerating and to recycling them, a very high chemical and thermal stability, and the easiness to synthesise them and obtain a very high conductivity. The advantage that the ionic liquids present is the possibility of changing their properties by varying the nature of the couple cation/anion [2,3].

Despite the studies on different generations of monocationic ionic liquids, there is still much to know about a wide variety of ionic liquids, especially in the case of dicationic ones.

Ionic liquids contain two head groups and two aliphatic chains linked by either a rigid or flexible connection. In addition to the combination of cation–anion, simple changes in the length of the bond or in the aliphatic chains of the cation are used to modify the physical properties of ionic liquids [4].

Dicationic ionic liquids are suitable candidates as advanced electrolyte materials in lithium ion batteries, fuel cells, dye-sensitised solar cells, and super capacitors [5–8,3]. In dicationic ionic liquids studied today, every dication is associated with two identical anions, which are either hydrophobic or hydrophilic. These ionic liquids are further classified as symmetric (the monocations that form the dication are the same) or asymmetrical (the monocations are different). There has been no report on the synthesis of dicationic ionic liquid, in which each dication is associated with two different anions, one hydrophobic and the other hydrophilic. By incorporating both hydrophilic and hydrophobic anions in dication, a further series of ionic liquid with properties that are different from existing ones are expected [9].

Dicationic ionic liquids are promising catalysts for the esterification reaction [10]. They have also been widely used in various fields of science because of their high thermal stability, a wide temperature range of the liquid state, and the biological activities such as antiviral, antifungal and anticancer activities. The ability of fictionalisation of dicationic ionic liquids gives the possibility of designing structures with respect to cations, anions and the length of the chain linking two cations, to achieve significant properties based on specific chemical tasks. In particular, the dicationic ionic liquids based on imidazolium and pyrrolidinium showed a variety of promising physicochemical properties in many applications [11].

FTIR/ATR and Raman spectroscopies are a vibrational spectroscopies technique that can provide a sensitive, relatively quick, non-destructive means of probing molecular structure in solid and liquid phases. It is also convenient for analysis of conformational dependence, and intra- and inter-chain interactions [12–16]. Numerous studies were performed on monocationic ionic liquids by FTIR/ATR and FT-Raman spectroscopies [1,17–21], but to the authors' knowledge, there does not exist at present a published FTIR and Raman spectroscopy study of dicationic ionic liquid behavior.

In this work, we present a comparative study by vibrational spectroscopies (FTIR/ATR and FT-Raman) between two ionic liquids; the first one is a dicationic ionic liquids that we have synthesised and characterised, and the second one is a monocationic ionic liquid, cited in the literature in the work of Noack et al. [1].

In this paper we use the [EMIM$^+$][NTf$_2^-$] notation instead of [C$_2$C$_1$IM$^+$][NTf$_2^-$] used in the previous Ref. [1].

2. Materials and methods

2.1. Reagents and materials

The reagents used in this study are, 1,2-diiodomethane, 1-methylimidazole (99 wt.%), (Acros), lithium bis(trifluoromethylsulfonyl)imide, diethylether and N,N-dimethylformamide, that were purchased from Fluka and used as received. Deionized H$_2$O was obtained with a Millipore ion-exchange resin deionizer.

2.2. NMR, spectroscopy analysis

^{1}H NMR (400 MHz), ^{13}C NMR, ^{19}F (100.6 MHz) spectra were recorded on DRX 400 MHz spectrometer. The chemical shifts (δ) are given in ppm and referenced to the internal solvent signal, TMS (Tetramethylsilane), and CFCl$_3$, respectively.

2.2.1. Synthesis and characterisation of bis-methyl imidazolium methylidene bis (trifluoromethanesulfonyl) imide

The synthesis of bis-methyl imidazolium methylidene bis (trifluoromethanesulfonyl) imide ionic liquid in the present study was based on a metathesis reaction of freshly prepared halide salts of the bis-methyl imidazolium alkylene cation and bis (trifluoromethylsulfonyl) imide as anions. An methylidene bis-methyl imidazolium iodide [M(CH$_2$)IM^{2+}][2I$^-$] was prepared by reacting of [(I(CH$_2$)I)] with two molar excess of 1-methylimidazole at 70 °C during 7 h.

In a round bottom flask, 1-methylimidazole (9.07 mL, 100 mmol) and 1,2-diiodomethane (5.07 mL, 50 mmol) were dissolved in toluene (15 mL) and the mixture was stirred at 70 °C for 5 h. The reaction mixture was evaporated under vacuum and the product washed with diethyl ether (5 × 20 mL). Bis-methyl imidazolium methylidene iodide yellowish solid (13.20 g, 31.86 mmol) was obtained in 73% yield. In Fig. 1, we present the protocole of the synthesis.

The reaction mixture was condensed by evaporation and the resultant solid was washed with diethylether to remove unreacted reagents. The ionic liquid was also subjected to anion exchange from Iodide to bis (trifluoromethane-sulfonyl) imide.

2.2.2. NMR results

The spectra details are given below,

^{1}H NMR (CDCl$_3$) δ ppm **[M(CH$_2$)IM^{2+}][2I$^-$]**: 3.05 (s, 6H, 2 × NCH$_3$), 6.09 (m, 2H, NCH$_2$N), 7.36 (m, 2H, NCHN), 7.73–7.49 (m, 4H, NCHCHN).

^{13}C NMR (CDCl$_3$) δ ppm **[M(CH$_2$)IM^{2+}][2I$^-$]**: 39.41, 51.66, 121.02, 123.23, 139.14, 139.96.

^{13}C NMR (CDCl$_3$) δ ppm **[M(CH$_2$)IM^{2+}]** [**2NTf$_2^-$**]: 37.24, 54.01, 120.43, 121.09, 135.12, 149.08.
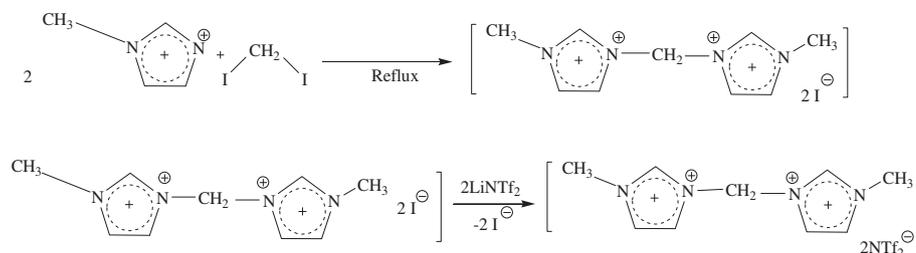
Fig. 1. Synthesis and structures of bis (trifluoromethanesulfonyl) imide bis-methyl imidazolium methylidene ionic liquid.

^{19}F NMR (CDCl$_3$) δ ppm **[M(CH$_2$)IM^{2+}]** **[2NTf$_2^-$]**: −77.23 (s, **CF$_3$SO$_2$)$_2$N**).

These results confirm the structure of our samples.

2.3. FTIR/ATR and FT-RAMAN measurements

The measurements were realised in the Walloon Agricultural Research Center (CRA-W) Belgium.

2.3.1. FTIR/ATR measurements

All attenuated total reflectance Fourier transform mid-infrared (ATR/FTIR) spectra were acquired on a Vertex 70-RAM II Bruker spectrometer (Bruker Analytical, Madison, WI) operating with a Golden Gate TM diamond ATR accessory (Specac Ltd., Slough, UK). FTIR/ATR spectra [4000–600 cm^{-1}] were collected with resolution of 1 cm^{-1} by co-adding 64 scans for each spectrum. The OPUS 6.0 software for windows of Bruker Instruments was used for instrument management.

2.3.2. FT-Raman measurements

FT-Raman spectra were acquired on a Vertex 70-RAM II Bruker FT-Raman spectrometer. This instrument is equipped with a Nd:YAG laser (yttrium aluminium garnet crystal doped with triply ionised neodymium) with a wavelength for the incident laser at 1064 nm (9398.5 cm^{-1}). The maximum laser power is 1.5 W. The measurement accessory is pre-aligned, only the Z-axis of the scattered light is adjusted to set the sample in the appropriate position regarding the local point. The RAM II spectrometer is equipped with a liquid-nitrogen cooled Ge detector. FT-Raman spectra [4000–45 cm^{-1}] were collected with resolution of 1 cm^{-1} by co-adding 128 scans for each spectrum. The OPUS 6.0 software was used for the spectral acquisition manipulation and transformation.

3. Results and discussion

3.1. Comparison between FTIR/ATR spectra of monocationic ([EMIM$^+$][NTf$_2^-$]) and dicationic ([M(CH$_2$)IM^{+2}][2NTf$_2^-$]) ionic liquids

In Fig. 2, we present the FTIR/ATR spectrum of ([M(CH$_2$)IM^{2+}][2NTf$_2^-$]) in the spectral range 3200–600 cm^{-1} and in Table 1 the observed FTIR/ATR bands and their assignment of ([EMIM$^+$][NTf$_2^-$]) (work of Noack et al. [1]) and ([M(CH$_2$)IM^{2+}][2NTf$_2^-$]) (this work).

From Table 1, we count 23 peaks for the monocationic and 44 peaks for the dicationic. The spectrum of the dicationic ionic liquid is richer in ways especially in the spectral range of 3000 cm^{-1}. We have a vaster spectral region (4000–600 cm^{-1}) than that studied by Noack et al. (4000–700 cm^{-1}).

In Fig. 3, we focused on the 1700–600 cm^{-1} FTIR spectral region.

3.1.1. Region 900–600 cm^{-1}

In this spectral region, bands appearing correspond to the ring and NC(H) bending mode of the imidaziolium cation. We also find
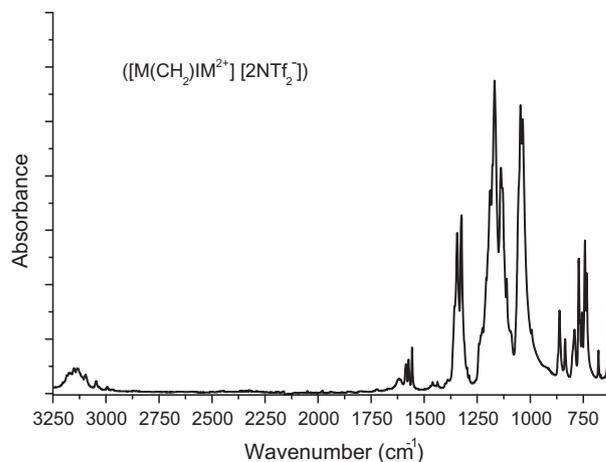
Fig. 2. FTIR/ATR spectrum of ([M(CH$_2$)IM^{2+}][2NTf$_2^-$]) in the spectral range 3200–600 cm^{-1}.

there the interaction with the anion at the wavenumber of 733 cm^{-1}. We note in this mode a slight wavenumber shift between mono and dicationic: about 4 cm^{-1}.

3.1.2. Region 1600–900 cm^{-1}

In this spectral region, we observe the most intense modes corresponding to the vibrations of the NTf$_2^-$ anion at 1040, 1140 and 1340 cm^{-1}. For the mono, we observe a peak in 1040 cm^{-1} with strong intensity while for the dicationic, we note a doublet 1035–1045 cm^{-1}. For 1140 cm^{-1} and 1340 cm^{-1}, we observe doublets in both cases but with wavenumber shift. For [EMIM$^+$] cation, we observe a doublet at 1135–1143 cm^{-1} while for the dicationic we note the same doublet at 1131–1138 cm^{-1} corresponding to a wavenumber shift of −4 cm^{-1}. For the monocationic 1332–1349 cm^{-1} passes to 1324–1344 cm^{-1} for the dicationic thus we observe a wavenumber shift of − 6 cm^{-1} and an enlargement of the doublet wavenumber pronounced with the appearance of a shoulder at 1355 cm^{-1}. This phenomenon could be explained by greater geometrical constraint in the case of dication.

The behavior of the mode at 1575 cm^{-1} differs a lot between the mono and the dicationic. In the first case, we have only a peak at 1575 cm^{-1} while in the second case we observe 3 peaks at 1557, 1573 and 1585 cm^{-1}. These bands are assigned to ring in-plane symmetric/anti-symmetric stretch CH$_2$(N) and CH$_3$(N)CN stretch. The connection CH$_2$(N) is more free in movements in the [EMIM$^+$] cation (connected with the CH$_3$—CH$_2$ (N)); however, in the [M(CH$_2$)IM^{2+}] cation this connection makes the link between both cations (N—CH$_2$—N) of a greater constraint which is translated by the appearance of new modes at 1557 and 1585 cm^{-1}. This mode serves as a marker of the change from mono to dicationic.

Table 1
Observed FTIR/ATR bands and their assignment of ([EMIM$^+$][NTf$_2^-$]) (work of Noack) and ([M(CH$_2$)IM^{2+}][2NTf$_2^-$]) (this work) at room temperature. vw = Very weak; w = weak; m = medium, s = strong; sh = shoulder; ν = Str = stretch; δ = deformation; bend = bending deformation; ω = wagging; ρ = rocking; s = symmetric; as = antisymmetric).

([EMIM$^+$] [NTf$_2^-$])	([M(CH$_2$)IM^{2+}] [2NTf$_2^-$])	Assignment	References
	605 (s)	ω(N—H)/CH$_3$(N)CN Str	[18]/[19]
	626 (m)	ω(N—H)/CH$_3$(N)CN Str	[18]/[19]
	678 (w)	ω(C—H) + ω(N—H)	[18]
714 (vw)	733 (m)	CH$_2$(N) and CH$_3$(N)CN str	[1]
729 (vw)		Anion interaction/ω(CH$_2$) rocking	[23]
	742 (m)	CF$_3$ sym bend ring	[1]
	755 (w)	ω(C—H)/SNS sym Str	[18]/[1]
762 (vw)	766 (w)	Δ(HCCH)/Ring HCCH asym bend	[17]/[1]
	771 (m)	ν(N—C)	[18]
790 (w)	791 (w)	Ring HCCH asym bend/CS Str	[1]
	835 (w)	NC(H)Nbend/CCHbend	[19]
845 (vw)		NC(H)Nbend/CCHbend	[19]
	861 (w)	ω(C—H) + ρ$_{as}$(CH$_2$)	[18]
	992 (w)	ρ$_{as}$(CH$_2$)	[15]
1040 (m)	1035(m) + 1045(m)	CH$_3$N Str/CH$_2$N Str, SO str	[1]
1055 (s)	1053 (sh)	CC str, NCH$_3$ twist, SNS asym str	[1]
	1090 (sh)	CC Str	[19]
	1110 (sh)	CC Str/δ(C—H)	[19]/[17]
1135(m) + 1143(m)	1131(m) + 1138(m)	SO$_2$ sym Str	[1]
1170 (s)	1168 (s)	CH$_2$(N) and CH$_3$(N)CN Str/CC Str	[1]
1184 (vs)	1188 (s)	CH$_3$(N)CN Str/CF$_3$ asym Str	[1]
1227 (w)	1225 (w)	ν(N—C)/CF$_3$sym Str	[18]/[1]
1240 (vw)	1242 (w)	Ring ip asym str, butyl chain str	[1]
	1288 (vw)	ρ(C—H)	[18]
	1297 (vw)	ν(C—C)	[18]
1332(w) + 1349(m)	1324(m) + 1344(m)	SO$_2$ asym str, CH$_2$(N),CH$_3$(N) CN str	[1]
	1355 (sh)	SO$_2$ asym str, CH$_2$(N),CH$_3$(N) CN str	[1]
1432 (vw)	1437 (vw)	CH$_3$(N)Str/CH$_3$(N)HCH sym bend	[1]
1455 (vw)	1460 (vw)	δ(CH$_2$)/CCH HCH asym bend	[16]/[19]
	1557 (w)	ν(N=C)	[18]
1575 (vw)	1573 (w)	Asym Str CH$_2$(N)/CH$_3$(N)CN Str	[1]
	1585 (w)	Asym Str CH$_2$(N)/CH$_3$(N)CN Str	[1]
	2967 (vw)	CH$_2$HCH asym Str	[1]
2990 (vw)	2994 (vw)	CH$_3$(N)HCH asym Str	[1]
	3028 (sh)	ν(C—H)	[18]
	3046 (w)	ν(C—H)	[18]
3105 (vw)	3096(w) + 3110(w)	ν(C—H)	[18]/[17]
3122 (vw)		ν(C—H)	[18]
	3132 (w)	Ring NC(H)NCH Str	[19]
	3150 (w)	C—H Str	[1]
3160 (vw)	3165 (w)	C—H Str	[1]
3174 (vw)	3173(w)	C—H Str	[1]
	3185(sh)	C—H Str	[1]
	3201 (sh)	ν(C—H)	[18]
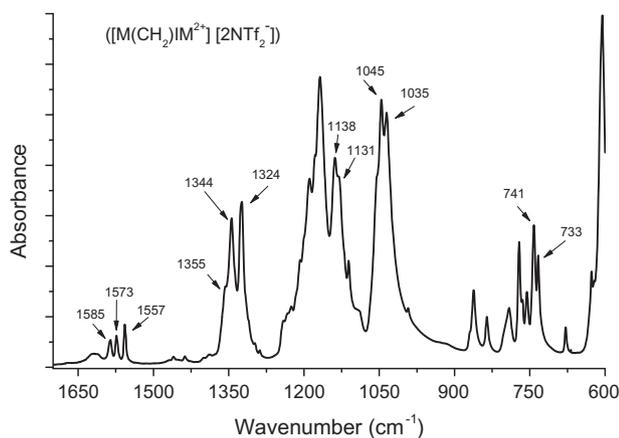
Fig. 3. FTIR/ATR spectrum of ([M(CH$_2$)IM^{2+}][2NTf$_2^-$]) in the spectral range 1700–600 cm^{-1}.
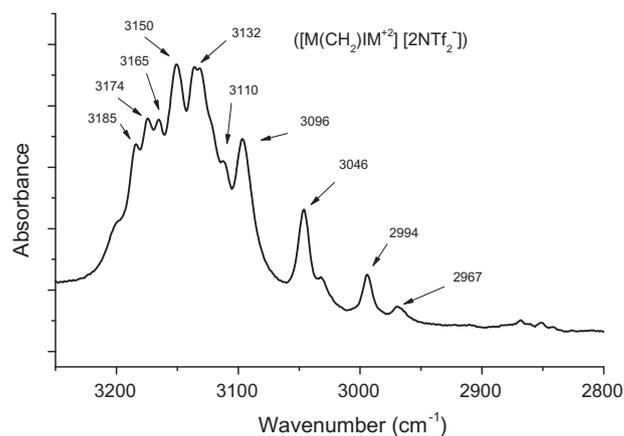
Fig. 4. FTIR/ATR spectrum of ([M(CH$_2$)IM^{2+}][2NTf$_2^-$]) in the spectral range 3250–2800 cm^{-1}.

3.1.3. Region 3250–2800 cm^{-1}

In Fig. 4, we present the FTIR/ATR spectrum of ([M(CH$_2$)IM^{2+}]-[2NTf$_2^-$]) in the spectral range 3250–2800 cm^{-1}. In this spectral region, we observe modes assigned the alkyl C—H stretching region. It is noticed that the spectrum which we obtained for the dicationic is much richer than that of the monocationic published

by Noack et al. [1]. Compared with the spectral region 1400–1000 cm^{-1}, the intensities of the modes are lower. The difference in behavior between mono and dication can be explained by an improved resolution of our device, either by enrichment of the modes directly related to the increase of the cation, or by both of them We observe new peaks well resolved for the dicationic: the modes at 2967 assigned to ν_{as}(CH$_2$HCH), 3046 to ν(C—H), 3132 to ν_{ring} (NC(H)NCH), 3150 to ν(C—H), 3185 and 3201 cm^{-1} to ν(C—H) [see Table 1]. We also observe a splitting between the mono and the dicationic: 3105 in 3096–3110 cm^{-1}. Among the peaks in common, there is a light wavenumber shift to 2990 cm^{-1} (against 2994 cm^{-1} for dicationic) to 3160 cm^{-1} (against 3165 cm^{-1} for the dicationic) and a peak which remains stable to 3174 cm^{-1}. So, we can conclude that this spectral region is also privileged to differentiate between mono and dicationic ionic liquids.

3.2. Comparison between FT-Raman spectra of monocationic ([EMIM$^+$][NTf$_2^-$]) and dicationic ([M(CH$_2$)IM^{2+}][2NTf$_2^-$]) ionic liquids

In Figs. 5–7, we present the FT-Raman spectrum of ([M(CH$_2$)-IM^{2+}][2NTf$_2^-$]) in the spectral ranges 950–45, 1700–1000 and 3200–2800 cm^{-1}, respectively. From Table 2, between our study
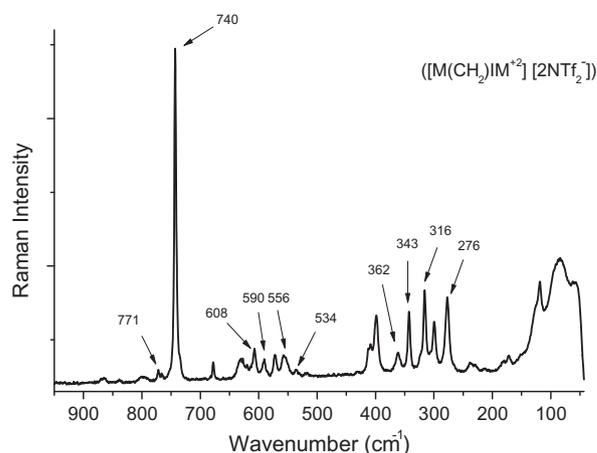
Fig. 5. FT-Raman spectra of ([M(CH$_2$)IM^{2+}][2NTf$_2^-$]) in the spectral range 950–45 cm^{-1}.

and that of Noack on FT-Raman, we notice that we have not the same spectral region of study: 3200–45 cm^{-1} for us and

Table 2
Observed FT-RAMAN bands and their assignment of ([EMIM$^+$][NTf$_2^-$]) (work of Noack) and ([M(CH$_2$)IM^{2+}][2NTf$_2^-$]) (this work) at room temperature. (vw = Very weak; w = weak; m = medium, s = strong; sh = shoulder; ν = Str = stretch; δ = deformation; bend = bending deformation; ω = wagging; s = symmetric; as = antisymmetric).

([EMIM$^+$][NTf$_2^-$])	([M(CH$_2$)IM^{2+}][2NTf$_2^-$])	Assignment	References
	57 (m)	Intermolecular vibration	[23]
	84 (m)	Intermolecular vibration	[23]
	119 (m)	Intramolecular vibration	[23]
	151 (vw)	Intermolecular vibration	[23]
	171 (vw)	ω(N—C)	[18]
	181 (vw)	Intermolecular vibration	[23]
	230 (vw)		
	238 (vw)		
262 (w)	276 (m)	CF$_3$ sym bending	[1]
303 (w)	300 (w)	CH$_2$(N)/CH$_3$(N)CH bend	[1]
	316 (m)	SC Str	[1]
	343 (w)	SC Str	[1]
	362 (vw)	SC Str	[1]
387	399(m) + 410(w)	CH$_2$(N), CH$_3$(N)CH bond, CH$_3$ bend	
534 (vw)	534 (vw)	SO$_2$ sym bending	[1]
	556 (vw)	SO$_2$ sym bending	
577 (w)	571 (w)	CH$_2$(N)/CH$_3$(N)CN Str	
	590 (w)	CH$_2$(N)/CH$_3$(N)CN Str	
	608 (vw)	ω(N—H/CH$_3$(N)CN Str	[18]/[20]/[19]
622	630 (vw)	ν(N—C)	[18]
687 (vw)	677 (vw)	CH$_2$(N)/CH$_3$(N)CN Str	
724 (vs)	744 (vs)	CF$_3$ sym str	
	771 (vw)	ρ(CH$_2$)rocking	[24]
942 (vw)		CC str	[1]
	992	ρ_{as}(CH$_2$)	[15]
1008 (w)	1016(w) + 1022(m) + 1029(w)	C—F sym str	[1]
	1046 (m)	ν(C—C)	[18]
1118 (w)	1111(w) + 1120(w) + 1134(m)	SO$_2$ sym str	
	1174 (vw)	SO$_2$ asym Str	[1]
1225 (m)	1242 (s)	SO$_2$ asym Str/CF$_3$ sym Str	[1]
1319 (w)	1324(w) + 1335(w)	SO$_2$ asym Str, CH$_2$(N)/CH$_3$(N)CN Str	[1]
	1361 (w)	ν(SO$_2$)	[21]
1378(vw) + 1407(w)	1399(sh) + 1413(w) + 1426(w)	CH$_2$(N)/CH$_3$(N)CN Str	[1]
1444 (w)	1461 (w)	CH$_3$(N)HCH sym bending	[1]
1553 (vw)	1572 (vw) + 1585 (vw)	CH$_2$(N)/CH$_3$(N)CN Str	[1]
	2838 (vw)	δ(CH$_3$)	[17]
	2967 (m)	ν_{as}(CH$_3$)	[15]
	2993 (w)	ν_{as}(CH$_3$)	[15]
	3028 (vw)	C—H Str/ν(C—H)	[24]/[18]
	3045 (vw)	ν(C—H)	[18]
	3096 (vw)	CH$_3$(N)HCH asym Str	[19]
	3135 (vw)	Ring NC(H)NCH Str	[19]
	3155 (vw)	Ring HCCH asym Str/ν(C—H)/	[19]/[18]/[25]
	3183 (vw)	ν(C—H)	[18]
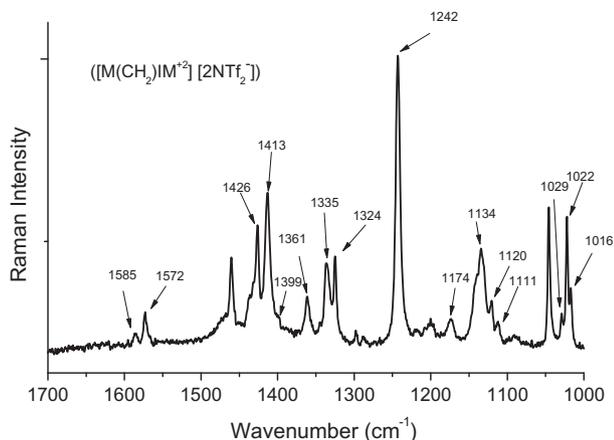
Fig. 6. FT-Raman spectrum of ([M(CH$_2$)IM^{2+}][2NTf$_2^-$]) in the spectral range 1700–1000 cm^{-1}.
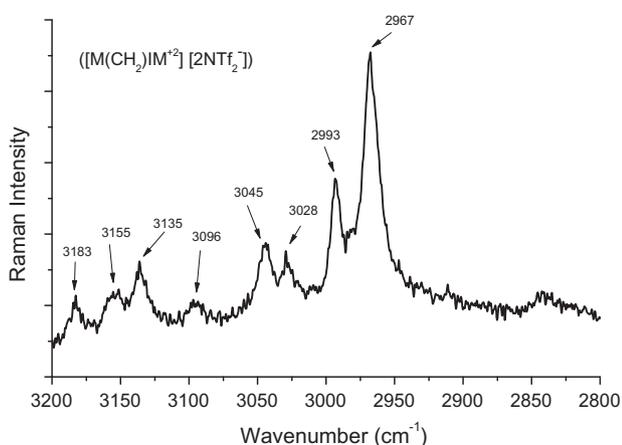
Fig. 7. FT-Raman spectrum of ([M(CH$_2$)IM^{2+}][2NTf$_2^-$]) in the spectral range 3200–2800 cm^{-1}.

1700–200 cm^{-1} for Noack. In the common region, our spectrum presents 19 new peaks with the passage from mono to dicationic. We can also notice a contrast between spectra in FT-Raman and in FTIR/ATR: there are many more active modes in FT-Raman than in FTIR/ATR.

3.2.1. Region 200–45 cm^{-1}

Bands appearing in this region correspond to the intermolecular and intramolecular vibrations with the NTf$_2^-$ anion [22,23]. We have here no elements of comparison between the mono and dicationic ionic liquids. Nevertheless, we can explore the vibrational behavior in this low frequency Raman region. Penna et al. [23] have observed at room temperature in this region for ionic liquids based on 1-alkyl-3methylimidazolium cations four components: 20, 70, 100 and 120 cm^{-1}. They have assigned 20, 70 and 100 cm^{-1} to intermolecular vibrational modes of NTf$_2^-$ anion and 120 cm^{-1} to an intramolecular normal mode of NTf$_2^-$ anion. For us, the component at ≈100 cm^{-1} is assigned to librational motion, i.e., hindered rotation, of the imidazolium ring because it is absent in non aromatic ionic liquids. The components observed at ≈20 cm^{-1} and ≈70 cm^{-1} at room condition are assigned to partial character of acoustic excitations because it is consistent with the fact that both of them are found independently of specific molecular structure either in aromatic or non aromatic ionic liquids and the dependence of the peak position with the strength of anion–cation interaction [23]. They have noted that when the sample at high pressure

crystallises, the librational component became a relativity sharp band at ≈140 cm^{-1} and one also saw another component at ≈185 cm^{-1}, which most probably is related to the shoulder at ≈150 cm^{-1} in the low temperature Raman spectrum. From Fig. 5, we observe in the low frequency Raman region six components: 57, 84, 119, 151, 171 and 181 cm^{-1}. The mode at 171 cm^{-1} is assigned to ω(N—C) [18]. From Penna's results [23], we can assign the modes at ≈57 cm^{-1} and ≈84 cm^{-1} to acoustic excitations, the mode at 119 cm^{-1} to an intramolecular normal mode of NTf$_2^-$ anion, and the modes at ≈141 cm^{-1} and ≈181 cm^{-1} to librational motion of the imidazolium ring. We also observe an important shift for the modes at ≈57 cm^{-1} and ≈84 cm^{-1} in comparison with the Penna's sample: from 20 cm^{-1} to 57 cm^{-1} and from 70 cm^{-1} to 84 cm^{-1}. These changes seem to be the consequence of the passage from one to two rings in the cation. The new geometrical constraints seem to have an impact on the intermolecular interactions and not on the intramolecular interactions because the mode at 120 cm^{-1} remains unchanged between both ionic liquids.

3.2.2. Region 1600–200 cm^{-1}

Bands appearing in this region are dominated by the contribution of the anion NTf$_2^-$ with remarkable changes between the mono and dicationic ionic liquids: 262 et 740 cm^{-1} assigned to CF$_3$ contributions, 316, 343, 362, 1016, 1022 et 1029 cm^{-1} assigned to CF contributions, and 534, 556, 1111, 1120, 1134, 1174, 1242, 1324, 1335 et 1361 cm^{-1} assigned to SO$_2$ contributions.

Between the passage of mono to dicationic for the contribution of the anion, we note the following new modes: 316, 343, 362, 556, 1174 and 1361 cm^{-1}. We observe splittings of peaks. The peak at 1008 cm^{-1} in the case of monocationic is transformed into a triplet for the dicationic: 1016, 1022 and 1029 cm^{-1} with a wavenumber shift of the order of +10 cm^{-1}; as well as for the peak at 1118 cm^{-1} which splits in 3 peaks: 1111, 1120 and 1134 cm^{-1}. For the peak at 1319 cm^{-1}, it is transformed into a doublet in the case of dicationic 1324 and 1335 cm^{-1} with a wavenumber shift of the order of +10 cm^{-1}. For peaks that do not undergo splitting, we observe important wavenumber shifts: 262–276 cm^{-1} (+14 cm^{-1}) and 1225–1242 cm^{-1} (+17 cm^{-1}). Only the peak in 534 cm^{-1} remains unchanged between the mono and the dicationic.

All this shows that the contribution of the anion is very sensitive to the changes of structure: the passage from a cation to a dication. These immediate changes of anion environment are directly translated by these wavenumber shifts, these spectral splittings and the appearance of new peaks.

In this spectral region, there is also the appearance of other peaks that are not related to the contribution of the anion: peaks at 590, 608, 771, 992 and 1046 cm^{-1}. The peak at 1046 cm^{-1} admits an important intensity. So, it could serve as a marker of differentiation between the mono and the dicationic. For the vibrational modes assigned to CH$_2$(N) and CH$_3$(N)CN stretch, we also observe an important splitting: the passage of the doublet 1378–1407 cm^{-1} to a triplet 1399–1413–1426 cm^{-1} with a wavenumber shift of +20 cm^{-1}.

There is also strong wavenumber shift for the peak at 1553 cm^{-1} because this one shifts nearly +20 cm^{-1} at 1572 cm^{-1}. A new peak at 1585 cm^{-1} also appears. As we observed in FTIR/ATR, these modes are markers of the change from mono to dicationic.

3.2.3. Region 3200–2800 cm^{-1}

In Fig. 7, we present the FT-Raman spectrum of ([M(CH$_2$)IM^{2+}] [2NTf$_2^-$]) in the spectral range 3200–2800 cm^{-1}. In this spectral region, we observe modes assigned to the alkyl C—H stretching region. We have no elements of comparison between the mono and dicationic in this spectral region. Compared with the spectral region 1400–1000 cm^{-1}, the intensities of the modes are a little

lower but compared with the same spectral zone in FTIR/ATR, we note that in FT-Raman with a length wave of the incident laser of 1064 nm the intensities of the modes are more important.

We can decompose this region into two ranges according to the spectra: 3000–2800 cm^{-1} and 3200–3000 cm^{-1}. In the first region, the vibrational modes of the CH$_3$ asymmetric stretch dominate: peaks at 2967 and 2993 cm^{-1}. In the second, we find the C—H stretching vibrational modes: 3028, 3045, 3096, 3135, 3155 and 3183 cm^{-1}.

4. Conclusion

In this study we have identified the main vibrational modes in FTIR/ATR and FT-Raman that differentiate between monocationic and dicationic ionic liquids almost similar (imidazolium ring and NTf$_2^-$ anion).

From this work, we note that the fact to take into account the two rings imidazolium in the ionic liquid is responsible of very important FTIR and FT-Raman vibrational changes. The more sensitive spectral regions concern 1600–900 cm^{-1} and 3200–2900 cm^{-1} for FTIR spectroscopy study, and 1700–200 cm^{-1} in comparison with the Noak's results. These changes reflect a movement and duplication or shift of some peaks in the case of dicationic ionic liquid which are explained by an effect of the number of the rings of the cation. All concerned modes could be like a marker of the differentiation between dicationic and monocationic ionic liquids. Especially, the peak appearing at 1046 cm^{-1} in FT-Raman of strong intensity which could be a very good witness of this differentiation.

Acknowledgment

References

[1] K. Noack, P.S. Schulz, N. Paape, J. Kiefer, P. Wasserscheid, A. Leipertz, Phys. Chem. Chem. Phys. 12 (42) (2010) 14153–14161.
[2] J.S. Wilkes, J. Mol. Catal. A: Chem. 214 (1) (2004) 11–17.
[3] F. Endres, S.Z. El Abedin, Phys. Chem. Chem. Phys. 8 (18) (2006) 2101–2116.
[4] B. Haddad, D. Villemin, E. Belarbi, N. Bar, M. Rahmouni, Arabian J. Chem., 2011.
[5] S. Seki, Y. Kobayashi, H. Miyashiro, Y. Ohno, A. Usami, Y. Mita, N. Kihira, M. Watanabe, N. Terada, J. Phys. Chem. B 110 (21) (2006) 0228–10230.
[6] N. Papageorgiou, Y. Athanassov, M. Armand, P. Bonho∕te, H. Pettersson, A. Azam, M. Grätzel, J. Electrochem. Soc. 143 (10) (1996) 3099–3108.
[7] A.B. McEwen, H.L. Ngo, K. LeCompte, J.L. Goldman, J. Electrochem. Soc. 146 (5) (1999) 1687–1695.
[8] M. Galiński, A. Lewandowski, I. St/kepniak, Electrochim. Acta 51 (26) (2006) 5567–5580.
[9] J.-C. Chang, W.-Y. Ho, I.-W. Sun, Y.-L. Tung, M.-C. Tsui, T.-Y. Wu, S.-S. Liang, Tetrahedron 66 (32) (2010) 6150–6155. août.
[10] A. Chinnappan, H. Kim, Chem. Eng. J. 187 (2012) 283–288.
[11] A.H. Jadhav, H. Kim, Chem. Eng. J. 200 (2012) 264–274.
[12] S. Bresson, M. El Marssi, B. Khelifa, Vib. Spectrosc. 40 (2) (2006) 263–269. mars.
[13] E. Da Silva, S. Bresson, D. Rousseau, Chem. Phys. Lipids 157 (2) (2009) 113–119. févr.
[14] S. Bresson, M.E. Marssi, B. Khelifa, Chem. Phys. Lipids 134 (2) (2005) 119–129. avr.
[15] M. El Hadri, A. Achahbar, J. El Khamkhami, B. Khelifa, V. Faivre, T.T. Cong, F. Bougrioua, S. Bresson, Vib. Spectrosc. 64 (2013) 78–88. janv.
[16] S. Bresson, D. Rousseau, S. Ghosh, M.E. Marssi, V. Faivre, Eur. J. Lipid Sci. Technol. 113 (8) (2011) 992–1004.
[17] A.M. Moschovi, S. Ntais, V. Dracopoulos, V. Nikolakis, Vib. Spectrosc. 63 (2012) 350–359. nov.
[18] K. Malek, A. Puc, G. Schroeder, V.I. Rybachenko, L.M. Proniewicz, Chem. Phys. 327 (2) (2006) 439–451.
[19] J. Kiefer, J. Fries, A. Leipertz, Appl. Spectrosc. 61 (12) (2007) 1306–1311.
[20] T. Buffeteau, J. Grondin, Y. Danten, J.-C. Lassègues, J. Phys. Chem. B 114 (22) (2010) 7587–7592.
[21] J.C. Lassegues, J. Grondin, R. Holomb, P. Johansson, J. Raman Spectrosc. 38 (5) (2007) 551–558.
[22] D. Xiao, L.G. Hines Jr., M.W. Holtz, K. Song, R.A. Bartsch, E.L. Quitevis, Chem. Phys. Lett. 497 (1-3) (2010) 37–42. sept.
[23] T.C. Penna, L.F.O. Faria, J.R. Matos, M.C.C. Ribiero, J. Chem. Phys. 138 (2013) 104503.
[24] G. Socrates, Infrared and Raman Characteristic Group Frequencies – Tables and Charts, third ed., J. Wiley & Sons, Chichester, 2001.
[25] T. Köddermann, C. Wertz, A. Heintz, R. Ludwig, ChemPhysChem 7 (9) (2006) 1944–1949.